HHS Public Access

Author manuscript

Hepatology. Author manuscript; available in PMC 2019 July 28.

Published in final edited form as:

Hepatology. 2018 March ; 67(3): 1071–1087. doi:10.1002/hep.29562.

Distinct Role of Nuclear Receptor Corepressor 1 Regulated *De Novo* Fatty Acids Synthesis in Liver Regeneration and Hepatocarcinogenesis in Mice

Qing Ou-Yang[1,2,3,*], **Xi-Meng Lin**[1,*], **Yan-Jing Zhu**[1,4,*], **Bo Zheng**[1,4,*], **Liang Li**[1,4], **Ying-Cheng Yang**[1], **Guo-Jun Hou**[1], **Xin Chen**[1,4], **Gui-Juan Luo**[1,4], **Feng Huo**[3], **Qi-Bin Leng**[5], **Frank J. Gonzalez**[6], **Xiao-Qing Jiang**[2], **Hong-Yang Wang**[1,4], **Lei Chen**[1,4,7]

[1]The International Cooperation Laboratory on Signal Transduction, Eastern Hepatobiliary Surgery Hospital, Second Military Medical University, Shanghai, China;

[2]Department of Biliary Surgery, Eastern Hepatobiliary Surgery Hospital, Second Military Medical University, Shanghai, China;

[3]Department of Hepatobiliary Surgery, Center of Liver Transplantation, General Hospital of Guangzhou Military Region, Guangzhou, China;

[4]National Center for Liver Cancer, Shanghai, China;

[5]Key Laboratory of Molecular Virology and Immunology, Institut Pasteur of Shanghai, Shanghai Institutes for Biological Sciences, Chinese Academy of Sciences, Shanghai, China;

[6]Laboratory of Metabolism, Center for Cancer Research, National Cancer Institute, National Institutes of Health, Bethesda, MD;

[7]Fudan University Shanghai Cancer Center; Department of Oncology, Shanghai Medical College, Fudan University, Shanghai 200032, China.

Abstract

It is urgent that the means to improve liver regeneration (LR) be found, while mitigating the concurrent risk of hepatocarcinogenesis (HCG). Nuclear receptor corepressor 1 (NCoR1) is a co-repressor of nuclear receptors, which regulates the expression level of metabolic genes; however, little is known about its potential contribution for LR and HCG. Here, we found that liver-specific *NCoR1* knockout in mice (*NCoR1*$^{\Delta hep}$) dramatically enhances LR after partial hepatectomy and, surprisingly, blocks the process of diethylnitrosamine (DEN)-induced HCG. Both RNA-sequencing and metabolic assay results revealed improved expression of *Fasn* and *Acc2* in

ADDRESS CORRESPONDENCE AND REPRINT REQUESTS TO: Lei Chen, Ph.D., International Co-operation Laboratory on Signal Transduction, Eastern Hepatobiliary Surgery Institute, Second Military Medical University, 225 Changhai Road, 200438 Shanghai, China, chenlei@smmu.edu.cn, Tel: 186-21-81875361; Hong-Yang Wang, M.D., Ph.D., International Co-operation Laboratory on Signal Transduction, Eastern Hepatobiliary Surgery Institute, Second Military Medical University, 225 Changhai Road, 200438 Shanghai, China, hywangk@vip.sina.com, Tel: 186-21-81875361; Xiao-Qing Jang, M.D., Department of Biliary Surgery, Eastern Hepatobiliary Surgery Hospital, Second Military Medical University, 225 Changhai Road 225, 200438 Shanghai, China, jxq1225@sina.com, Tel: 186-21-81875361.

*These authors contributed equally to this work.

Potential conflict of interest: Nothing to report.

Supporting Information

Additional Supporting Information may be found at onlinelibrary.wiley.com/doi/10.1002/hep.29562/suppinfo.

NCoR1$^{\Delta hep}$ mice, suggesting the critical role of *de novo* fatty acid synthesis (FAS) in LR. Continual enhanced *de novo* FAS in *NCoR1*$^{\Delta hep}$ mice resulted in overwhelmed adenosine triphosphate ATP and nicotinamide adenine dinucleotide phosphate (NADPH) consumption and increased mitochondrial reactive oxygen species production, which subsequently attenuated HCG through inducing apoptosis of hepatocytes at an early stage after DEN administration. *Conclusion*: NCoR1 functions as a negative modulator for hepatic *de novo* FAS and mitochondria energy adaptation, playing distinct roles in regeneration or carcinogenesis.

The liver has a remarkable capacity for regeneration after injury.[1,2] Sustained liver reparation and regeneration triggered by chronic liver injury can bring about genetic mutations and induce hepatocarcinogenesis (HCG).[3,4] However, the signals that initiate or terminate hepatocyte proliferation are still incompletely defined.[5,6]

Nuclear receptor corepressor 1 (NCoR1) serves as a cofactor that facilitates the interaction of several nuclear proteins that regulate the transcription rates of metabolic stress-induced genes.[7,8] Interactions between NCoR1, nuclear receptors and deacetylases, and transducing beta-like 1 has been studied, and it has been found that they can form a co-repressor complex for the down-regulation of target genes.[9–11] Expression of their target genes is increased in the absence of NCoR1, which confirms the important role that NCoR1 has in controlling the amplitude of nuclear receptors.[10] Interestingly, steatosis was also observed in *NCoR1* hepatic knockout (*NCoR1*$^{\Delta hep}$ mice.[9] Thus, disrupting *Ncor1 expression* could up-regulate the expression of metabolic genes, such as lipogenesis genes and lipid oxidation genes.[12]

Lipid metabolism was identified as playing a major role in the regulation of liver regeneration (LR) and HCG.[13] Peripheral lipid mobilization was determined to be indispensable for the initiation of LR.[2] Improved lipid metabolism in chronic liver diseases, such as nonalcoholic steatohepatitis (NASH), was found to have a promoting role in hepatocellular carcinoma (HCC).[14] Taken together, these observations suggest that enhanced lipid metabolism induced by liver injury is involved in the compensatory proliferation and development of HCC. However, hampering lipogenesis could also promote tumor growth, as evidenced by the results of knockdown of acetyl-CoA carboxylases (ACCs) ACC1 or ACC2, a key enzyme of lipogenesis that facilitates cancer cell survival and tumor formation.[15]

Based on the intriguing relationship between NCoR1 and lipid metabolism, as revealed in previous studies, the current work was undertaken to assess the influence of liver-specific disruption of *NCoR1* on compensatory proliferation after partial hepatectomy (PH) and HCG.

Materials and Methods

The full materials and methods are available in the Supporting Information.

GENERATION OF *NCoR1*$^{\Delta hep}$ MICE

NCoR1 floxed (*NCoR1*$^{fl/fl}$) and albumin (*Alb*)-Cre mice (*Alb*-creTg/0) were generated as described using the Cre-loxP system.[16] Briefly, offspring that transmitted the mutated allele, in which the selection marker was excised, and that lost the Flp transgene (*NCoR1*$^{L2/WT}$ mice) were selected, mated with mouse *Alb*-Cre mice, and then further intercrossed to generate mutant (*Alb*)-creTg/0/-*NCoR1*$^{L2/L2}$ mice, which were termed *NCoR1*$^{\Delta hep}$ mice. *NCoR1*$^{\Delta hep}$ mice, back-crossed for over 10 generations to C57BL/6J, were used in experiments with *NCoR1*$^{fl/fl}$ used as controls (Supporting Fig. S1B,C).

ANIMALS AND EXPERIMENTAL PROCEDURES

All animal experiments were performed in accord with the National Institutes of Health guidelines and approved by the Animal Care and Use Committee of the Second Military Medical University (Shanghai, China). PH surgeries were performed in 8- to 12-week-old mice by removal of two thirds or one third of the liver as described.[17] For diethylnitrosamine (DEN)-induced HCG, mice at day 15 of age were injected intraperitoneally with DEN (10 mg/kg, intraperitoneally) diluted in saline buffer. GW6471 (peroxisome proliferator-activated receptor [PPAR]α antagonist) was injected intraperitoneally (1 mg/kg, intraperitoneally). Adeno-associated virus (AAV) was diluted in phosphate-buffered saline (PBS) and injected through the caudal vein (virus titer, 10^{11}/mL, 200 μL/mouse). For more information, please see the Supporting Information.

STATISTICAL ANALYSIS

All data in this study represent at least three experiments and are expressed as the mean ± SEM. Differences between groups were compared using the Student *t* test or two-way analysis of variance (as indicated in each figure/table). Statistical significance was determined as $P < 0.05$. Analysis was performed using GraphPad Prism software (GraphPad Software Inc., San Diego, CA).

Results

ENHANCED CELL PROLIFERATION IN *NCoR1*$^{\Delta hep}$ MICE AFTER PH

We performed two-thirds PH on *NCoR1*$^{fl/fl}$ mice and *NCoR1*$^{\Delta hep}$ mice. NCoR1 protein levels rapidly reduced at 24 hours post-two-thirds PH, but rebounded at 48 hours after two-thirds PH (Fig. 1A). *NCoR1* mRNA expression was also down-regulated after two-thirds PH (Fig. 1B). The change of liver/body weight ratio in *NCoR1*$^{fl/fl}$ and *NCoR1*$^{\Delta hep}$ mice during the process of LR revealed that restoration of liver/body weight ratios in *NCoR1*$^{\Delta hep}$ mice occurred much earlier and faster than in *NCoR1*$^{fl/fl}$ mice. The same result was observed in one-third PH models. However, liver/body weight ratios of *NCoR1*$^{fl/fl}$ mice were similar to that of *NCoR1*$^{\Delta hep}$ mice at 5–7 days post-two-thirds PH (Fig. 1C). In the process of sample collection, liver mass of *NCoR1*$^{\Delta hep}$ mice was larger than *NCoR1*$^{fl/fl}$ mice at 96 hours post-two-thirds PH (Fig. 1D). More vacuolated and swelling hepatocytes were observed in livers of *NCoR1*$^{\Delta hep}$ mice, even at 96 hours after two-thirds PH, as revealed by hematoxylin-eosin (H&E) staining (Fig. 1D). In the next step, immunohistochemical (IHC) analysis of Ki67, a marker of cell-cycle entry, was detected. The result revealed that more Ki67-positive cells

were observed at 48 hours post-two-thirds PH in *NCoR1*$^{\Delta hep}$ mice compared to *NCoR1*$^{fl/fl}$ mice. At 96 hours post-two-thirds PH, some Ki67-positive cells were still observed in livers of *NCoR1*$^{\Delta hep}$ mice, coincident with higher and prolonged cell mitosis (Fig. 1E). Pathway analysis of cell-cycle-related proteins revealed an earlier induction of Cyclin D1 (marker of G1/S) at the initial time and even higher expression at 96 hours post-two-thirds PH (Fig. 1F). In agreement with morphology results, enhanced expression of Cyclin A2 (marker of G2/M or mitosis) at 48 hours post-two-thirds PH and prolonged expression of Cyclin B1 (marker of G2/M) and proliferating cell nuclear antigen (PCNA) was observed (Fig. 1F). A similar tendency was noted on mRNA levels (Supporting Fig. S1A). Because cell-cycle inhibitors P21 and P27 are known to inhibit CCND1-CDK4 complex activity, we further examined the expression change of P21 and P27 proteins during LR and found that the protein level of P27 was dramatically decreased in *NCoR1*$^{\Delta hep}$ mice (Supporting Fig. S1F). These results indicate that hepatic NCoR1 deficiency contributed to enhanced LR after two-thirds PH, at least partly through modulating cell-cycle entry.

BIOINFORMATICS ANALYSIS OF NCoR1 TARGET GENES ACCOUNTED FOR THE ENHANCEMENT OF COMPENSATORY PROLIFERATION IN *NCoR1*$^{\Delta hep}$ MICE

In order to find the specific target genes of NCoR1 that play a key role in regulating the enhancement of compensatory proliferation in *NCoR1*$^{\Delta hep}$ mice at an early stage, liver tissues were collected from *NCoR1*$^{fl/fl}$ and *NCoR1*$^{\Delta hep}$ mice at 0, 24, and 48 hours after two-thirds PH and an RNA-sequencing was carried out. Obvious differences in cellular morphology and molecular study were discovered at indicated time points. Analysis of differences existing in the expression of genes at the three indicated times between two groups showed that metabolism-related genes may have had a dominant role in regulating regenerative capacity of hepatocytes (Fig. 2A,C). At 0 and 48 hours after two-thirds PH, 45 genes in *NCoR1*$^{\Delta hep}$ were observed to be exclusively up-regulated compared to *NCoR1*$^{fl/fl}$ mice by intergroup comparison (Fig. 2D). Furthermore, these genes were mostly fatty acid synthesis (FAS)-related genes (Fig. 2D). Gene coexpression network analysis showed that the genes in the central node of the network have a large number of connections, such as acetyl-CoA carboxylase 2 (*Acacb*, *Acc2*) and fatty acid synthase (*Fasn*; Fig. 2E). ACC2 is a rate-limiting enzyme in *de novo* FAS, but is normally expressed in myocytes and not hepatocytes (Fig. 2F). Furthermore, FASN plays a pivotal role in many process of *de novo* FAS (Fig. 2F). qPCR assay further confirmed elevation of glucose transport type 4 (*Glut4*), glucose-6-phosphate dehydrogenase (*G6pd*), *Fasn*, and *Acc2* genes in *NCoR1*$^{\Delta hep}$ mice compared to *NCoR1*$^{fl/fl}$ mice (Fig. 2G).

Because NCoR1 binds to nuclear receptors to repress the transcriptional activity of target genes, several published hepatic NCoR1 chromatin immunoprecipitation sequencing (ChIP-seq) data sets were retrieved in order to find the specific NCoR1 target genes (Gene Expression Omnibus, GSM647027 and GSM647028). In addition, genes were defined that they have peaks within 3,000 base pairs around the transcriptional start site, and this may represent NCoR1 target genes. Therefore, these 45 genes near NCoR1-binding sites were checked from two ChIP-seq results in liver (day and night, 10:00 AM and 10:00 PM). ChIP-seq results showed that *Fasn* and *Acc2* were potential NCoR1 target genes in normal mice without surgery (Fig. 2I). This result was also verified by ChIP-qPCR with antibody of

NCoR1 and Control, only NCoR1 antibody could directly combined with sequence of promoter region of Fasn and Acc2 (Fig. 2J).

ACC1, ACC2, and FASN are three rate-limiting enzymes of *de novo* FAS, but unlike ACC1, ACC2 usually expresses in heart and muscle, which regulates a bypass of *de novo* FAS and could inhibit fatty acid β-oxidation (FAO) by indirectly regulating carnitine palmitoyltransferase 1 (CPT1; Fig. 2F). Thus, ACC2 could facilitate lipid accumulation more effectively. Interestingly, the western blotting results showed that the expression peak of ACC2 came earlier in $NCoR1^{\Delta hep}$ mice than $NCoR1^{fl/fl}$ mice and disappeared rapidly in both groups (Fig. 2H). Expression of FASN in $NCoR1^{\Delta hep}$ mice was up-regulated at 0 hours and decreased quickly, whereas it hit its expression peak at 24 hours and maintained a stable level in $NCoR1^{fl/fl}$ mice (Fig. 2H). A recent article documented that acetylation of FASN is positively correlated with degradation of FASN through the ubiquitin-proteasome pathway.[18] The effect of acetylation of FASN is may be occurred in deficiency of NCoR1, as NCoR1 plays a role of deacetylation by cooperation with HDAC3.[10] We thus examined the expression level of the specific acetylase, lysine acetyltransferase 8 (KAT8), and the deacetylase, histone deacetylase 3 (HDAC3), targeting FASN. Interestingly, Fig. 2K shows that KAT8 is comprehensively up-regulated in $NCoR1^{\Delta hep}$ mice and HDAC3 is down-regulated in $NCoR1^{\Delta hep}$ mice, which implied that the intracellular balance of KAT8 and HDAC3 is necessary for protein level of FASN.

To further verify the direct contribution of ACC2 for LR, adeno-associated virus (AAV-ACC2-shRNA [small hairpin RNA]) targeting expression of ACC2 in liver was applied before PH in $NCoR1^{fl/fl}$ or $NCoR1^{\Delta hep}$ mice by caudal vein injection (knockdown efficiency was verified by the real-time PCR method, as shown in Supporting Fig. S5A). Figure 2L shows that knockdown expression of ACC2 significantly retarded the proliferative rate of hepatocytes in $NCoR1^{\Delta hep}$ mice, and a similar regeneration curve was found in both $NCoR1^{\Delta hep}$ and $NCoR1^{fl/fl}$ mice after PH. It should be noted that administration of AAV-ACC2-shRNA could not completely block hepatocyte proliferation, and a slight increase in regeneration rate in $NCoR1^{\Delta hep}$ mice was observed in the absence of ACC2 (24 and 48 hours post-PH in Fig. 2L). These results indicate that deficiency of NCoR1 may facilitate *de novo* FAS in the early stage of LR by up-regulating the expression of specific genes involved in lipid metabolism at the 0 time point, such as *Fasn* and *Acc2*.

ENHANCED *DE NOVO* FAS, GLUCOSE FLUX, MITOCHONDRIAL FUNCTION FOLLOWING PH IN $NCoR1^{\Delta hep}$ MICE

In order to verify whether enhanced *de novo* FAS, predicted by bioinformatics analysis, does exist in the two-thirds PH model of $NCoR1^{\Delta hep}$ mice, Oil Red O staining for these tissue sections was detected and the result showed increased accumulation of lipid droplets, which was correlated with transient elevated triglyceride (TG) levels in livers of $NCoR1^{\Delta hep}$ mice compared to $NCoR1^{fl/fl}$ mice (Fig. 3A,B). The accumulation of lipid drops may come from two different sources: (1) from glucose by *de novo* FAS and (2) from fatty acids by peripheral fat mobilization. In order to determine which process was influenced by NCoR1 deficiency, we detected the glucose level in serum and the change ratio of body weight in the process of LR. $NCoR1^{\Delta hep}$ mice showed a lower serum glucose level in each time point, but

with less weight loss, compared to *NCoR1*$^{fl/fl}$ mice (Fig. 3B; Supporting Table S1). In addition, because it was determined that one-third PH induced less stimulus and peripheral lipid mobilization in the process of LR,[28] we performed a one-third PH in *NCoR1*$^{fl/fl}$ and *NCoR1*$^{\Delta hep}$ mice. More lipid accumulation in 36 hours after one-third PH was observed in *NCoR1*$^{\Delta hep}$ mice (Fig. 4E,G). These results indicate that increased lipid drops at 24 hours after two-thirds PH in *NCoR1*$^{\Delta hep}$ mice may be regulated by enhanced *de novo* FAS, which is correlated with advanced expression of FASN and ACC2 in *NCoR1*$^{\Delta hep}$ at the initial time.

Because enhanced *de novo* FAS is associated with glucose flux, expression of proteins regulating glucose metabolism was measured during the process of LR. Up-regulation of GLUT4 and G6PD was observed during LR, which was correlated with a lower serum glucose level in *NCoR1*$^{\Delta hep}$ mice (Fig. 3B,C). Enhanced glucose flux and mitochondrial activity could be induced by NCoR1 deficiency because more glucose and adenosine triphosphate (ATP) consumption are required for *de novo* FAS (Fig. 2F). To confirm this, glucose metabolism was measured by using the Seahorse analyzer to detect the O_2 consumption rates and H^+ production of primary hepatocytes from *NCoR1*$^{\Delta hep}$ and *NCoR1*$^{fl/fl}$ mice. Deficiency of NCoR1 increased both the basal and maximal oxidative phosphorylation capacity, as indicated by rising O_2 consumption (Fig. 3D). However, even though the glycolytic capacity of primary hepatocytes from *NCoR1*$^{\Delta hep}$ mice was similar to *NCoR1*$^{fl/fl}$ mice, elevated glycolytic capacity was noted with glucose and oligomycin (a mitochondrial inhibitor) treatment (Fig. 3D). The result indicated that more glucose and energy is required for *NCoR1*$^{\Delta hep}$ hepatocytes. Then, the protein levels of C-MYC and retinoblastoma protein (p-RB) were found to be up-regulated, which is closely related to metabolism and mitosis in the process of LR (Fig. 3C).

Enhancement of *de novo* FAS could induce more ATP consumption, but more lipids could provide more ATP through FAO (Fig. 2F). To confirm the energy state during the regeneration process, intracellular ATP levels in *NCoR1*$^{fl/fl}$ and *NCoR1*$^{\Delta hep}$ mice at the early stages of LR were examined. At the 0 point, deficiency of NCoR1 was associated with increased intracellular ATP levels (Fig. 3E). Although ATP levels were decreased 24 hours after PH, which might result from the rapid production of lipids consuming more ATP transiently, a faster and stronger increase of ATP level was observed in *NCoR1*$^{\Delta hep}$ mice 48 hours after PH (Fig. 3E). These data suggest that deficiency of NCoR1 could enhance glucose flux and *de novo* FAS effectively in the short term and consequently provide more energy during the process of LR.

G6PD, a key enzyme in the pentose phosphate pathway (PPP), was up-regulated in *NCoR1*$^{\Delta hep}$ mice during LR (Fig. 3C). The PPP is the major production source of $NADP^+$ reduced (NADPH), which is an indispensable reducing substance for consumption in *de novo* FAS (Fig. 2F). Enhancement of *de novo* FAS in deficiency of NCoR1 may also influence the NADPH level and redox state. We thus examined the nicotinamide adenine dinucleotide phosphate ($NADP^+$)/NADPH ratios and mitochondrial reactive oxygen species (ROS) in *NCoR1*$^{fl/fl}$ and *NCoR1*$^{\Delta hep}$ mice after two-thirds PH. Interestingly, higher levels of $NADP^+$/NADPH ratio and mitochondrial ROS were observed in *NCoR1*$^{\Delta hep}$ mice, but not *NCoR1*$^{fl/fl}$ mice (Fig. 3E). These data imply that enhancement of *de novo* FAS in the absence of NCoR1 may not only lead to consumption of NADPH (Fig. 2F) and

mitochondrial reactive oxygen species (ROS) enrichment, but also induces compensatory reprogramming of the metabolic state, such as enhancing the G6PD-dependent PPP process to generate NADPH.

ENHANCEMENT OF *DE NOVO* FAS FACILITATES COMPENSATORY PROLIFERATION IN LIVER OF *NCoR1*$^{\Delta hep}$ MICE

In order to determine whether enhancement of *de novo* FAS facilitated compensatory proliferation in liver, we treated *NCoR1*$^{fl/fl}$ and *NCoR1*$^{\Delta hep}$ mice with a selective FASN inhibitor (orlistat) intraperitoneally at the indicated time point (Fig. 4A). As expected, no significant differences of liver/body weight ratio, Ki67, and lipid in oil staining, together with Cyclin D1 expression, were observed between *NCoR1*$^{fl/fl}$ and *NCoR1*$^{\Delta hep}$ mice after orlistat treatment (Fig. 4A–C). We also detected the effect of orlistat on hepatic TG concentration, body weight change ratio, and serum glucose level at indicated times after two-thirds PH (Fig. 4D), and found that orlistat attenuated the accumulation of TG at an early stage in both wild-type and knockout mice. The effects of NCoR1 depletion causing differences in body weight change ratio and serum glucose between *NCoR1*$^{fl/fl}$ and *NCoR1*$^{\Delta hep}$ mice were eliminated upon orlistat treatment. These data suggested that orlistat could effectively inhibit *de novo* FAS in liver, which plays a pivotal role in enhanced LR in *NCoR1*$^{\Delta hep}$ mice.

To further confirm that inhibiting *de novo* FAS could hamper the energy production and disturb redox homeostasis during LR, intracellular ATP levels in *NCoR1*$^{fl/fl}$ and *NCoR1*$^{\Delta hep}$ mice pretreated with orlistat at 24 hours before and after two-thirds PH were measured. Deficiency of NCoR1 increased intracellular ATP levels at 24 hours after orlistat injection (Supporting Fig. S2A). However, at 48 hours after two-thirds PH, there was little difference of ATP level between the two mouse lines (Supporting Fig. S2A). This phenomenon indicates that the extent of lipid accumulation is associated with initiation of mitosis. Thus, inhibiting *de novo* FAS may delay LR because of less ATP supply. We also detected the $NADP^+$/NADPH ratios and mitochondrial ROS in *NCoR1*$^{fl/fl}$ and *NCoR1*$^{\Delta hep}$ mice pretreated with orlistat at indicated times after two-thirds PH. The results showed that even though $NADP^+$/NADPH ratios and mitochondrial ROS levels were up-regulated in *NCoR1*$^{\Delta hep}$ mice compared to *NCoR1*$^{fl/fl}$ mice, they were down-regulated after orlistat treatment. At 48 hours after two-thirds PH, $NADP^+$/NADPH ratios and mitochondrial ROS levels were still higher than normal condition in both mouse lines (Supporting Fig. S2B, C). These results indicated that enhanced *de novo* FAS might result in a short-term oxidative stress in liver after two-thirds PH, and inhibiting *de novo* FAS not only delayed the hepatocyte mitosis, but also the recovery of redox state.

To exclude the possible effect of exogenous lipid on hepatocyte proliferation in our study, we performed a one-third PH in *NCoR1*$^{fl/fl}$ and *NCoR1*$^{\Delta hep}$ mice, which is a typical model with less stimulus and peripheral lipid mobilization in the process of LR (Fig. 4F).[28] We found earlier restoration of liver size and appearance of Ki67 staining-positive cells 36 hours after one-third PH in *NCoR1*$^{\Delta hep}$ mice (Fig. 4G). Additionally, survival and growth rate of *NCoR1* knockdown cells were faster than control cells upon exogenous fatty acid deprivation (Dulbecco's modified Eagle's medium [DMEM] with 1% fetal bovine serum

[FBS]). However, similar results were not found in normal culture medium (DMEM with 5% FBS; Supporting Fig. S3C–E). These data indicate that NCoR1 deficiency could provoke hepatocyte survival and proliferation through enhancing *de novo* FAS, but not mobilizing peripheral lipid.

DEFICIENCY OF NCoR1 ATTENUATED HCG IN DEN-INDUCED HCC MODEL

Higher metabolic rate and regenerative capacity in NCoR1 knockout hepatocytes than $NCoR1^{fl/fl}$ hepatocytes prompted us to explore the propensity of carcinogenesis of NCoR1 deficiency. Twenty-month-old $NCoR1^{\Delta hep}$ mice showed no lesion of tumor without other intervention (data not shown). When we submitted 15-day-old $NCoR1^{fl/fl}$ and $NCoR1^{\Delta hep}$ mice to an acute treatment of DEN, a larger number of vacuolated lesions were observed in livers of $NCoR1^{\Delta hep}$ mice in H&E staining, which indicated a more-severe response to DEN (Fig. 5B). However, 12 weeks after DEN treatment, the liver/body weight ratio increased far more in $NCoR1^{\Delta hep}$ mice than $NCoR1^{fl/fl}$ mice and with more swelling hepatocytes in H&E staining (Fig. 5A,B). Interestingly, $NCoR1^{fl/fl}$ mice developed mac-roscopically visible tumors 30 weeks after DEN treatment, which were barely observed in $NCoR1^{\Delta hep}$ mice (Fig. 5A). At 36 weeks after DEN treatment, numerous tumor nodules were observed in whole liver of $NCoR^{fl/fl}$ mice, whereas few lesions of tumor were discovered in $NCoR1^{\Delta hep}$ mice with decreased liver/body weight ratio (Fig. 5A,C). The obvious morphology change of swelling observed at the early stage after DEN treatment in $NCoR1^{\Delta hep}$ mice may be associated with lipid accumulation and DNA damage. Hence, we detected TG and 8-hydroxy-2′-deoxyguanosine (8-OHdG; 8-OH) level in livers 4 weeks after DEN treatment. A higher level of TG was detected in $NCoR1^{\Delta hep}$ mice than in $NCoR1^{fl/fl}$ mice (Fig. 5D). DEN increased 8-OHdG (an indicator of ROS-induced DNA damage) level in both $NCoR1^{\Delta hep}$ mice and $NCoR1^{fl/fl}$ mice, and we found that expression level of 8-OHdG was significantly improved in $NCoR1^{\Delta hep}$ mice (Fig. 5D). Furthermore, we detected the expression change of key proteins of *de novo* FAS (Fig. 2F) with or without DEN treatment 4 weeks after DEN treatment in $NCoR1^{fl/fl}$ and $NCoR1^{\Delta hep}$ mice. The result showed that the level of ACC2, FASN, GLUT4, and G6PD were higher in $NCoR1^{\Delta hep}$ mice than $NCoR1^{fl/fl}$ mice, even though DEN treatment could elevate their expression slightly (Fig. 5E). These results indicate that a chronic injury induced by DEN treatment could cause a higher level of *de novo* FAS and that NCoR1 deficiency might have attenuated the propensity of carcinogenesis after DEN treatment.

NCoR1 DEFICIENCY ENHANCES THE OXIDATIVE STRESS LEVEL AND HEPATOCYTE APOPTOSIS AFTER DEN TREATMENT

High expression levels of 8-OHdG (8-OH) and G6PD protein were observed in DEN-treated $NCoR1^{\Delta hep}$ mice at an early stage (Fig. 5E); we thus speculated that such prolonged *de novo* FAS in $NCoR1^{\Delta hep}$ mice may consume much more NADPH provided by the PPP pathway (Fig. 2F). Consistently, expression level of G6PD was still high 4 weeks after DEN treatment in $NCoR1^{\Delta hep}$ mice (Fig. 5E). These events may have resulted in an imbalance of the redox state in the liver given that NADPH was insufficient. In order to demonstrate this consequence of long-term FAS after DEN treatment, $NADP^+$/NADPH ratio, glutathione disulfide (GSSG)/glutathione (GSH) ratio, and mitochondrial ROS were measured 4 weeks after DEN treatment. As expected, $NADP^+$/NADPH and GSSG/GSH ratios and levels of

mitochondrial ROS were increased in *NCoR1*$^{\Delta hep}$ mice compared to *NCoR1*$^{fl/fl}$ mice after DEN treatment (Fig. 6A). Meanwhile, ATP level was reduced in liver compared to *NCoR1*$^{fl/fl}$ mice 4 weeks after DEN treatment (Fig. 6A). These results indicate that DEN-treated *NCoR1*$^{\Delta hep}$ mice may suffer from more-severe oxidative stress and NADPH consumption than control mice.

Generally, oxidative stress and DNA damage could induce apoptosis. This may explain the phenomenon that less tumor was formed in *NCoR1*$^{\Delta hep}$ mice after DEN treatment if apoptosis was enhanced. Indeed, morphological studies showed persistent cell apoptosis and DNA damage 4 weeks after DEN treatment in *NCoR1*$^{\Delta hep}$ mice, but not in *NCoR1*$^{fl/fl}$ mice, as revealed by TUNEL (terminal deoxynucleotidyl transferase dUTP nick end labeling) and 8-OHdG staining, respectively (Fig. 6B). In *NCoR1*$^{\Delta hep}$ mice without DEN treatment, TUNEL staining-positive cells were not observed (data not shown). In addition, higher levels of Oil Red O staining were observed 4 weeks after DEN treatment (Fig. 6B). Ki67 staining was weakly positive in a number of hepatocytes in *NCoR1*$^{\Delta hep}$ mice, but not in *NCoR1*$^{fl/fl}$ mice (Fig. 6B). In order to determine that the increased cell apoptosis was induced by over-reinforced *de novo* FAS in *NCoR1*$^{\Delta hep}$ mice, we administered orlistat, a selective inhibitor of *de novo* FAS, in two groups of mice after DEN treatment. Orlistat administration was provided 5 days before sample collection 4 weeks after DEN treatment. Notably, orlistat treatment clearly abrogated the distinct levels of TUNEL, 8-OHdG, Oil Red O, and Ki67 staining between the two groups of mice after DEN administration (Fig. 6B). In addition, expression of P53 and protease-activated receptor 4 (PAR4), genes related to apoptosis, was up-regulated in NCoR1-deficient livers 4 weeks after DEN treatment (Fig. 6C). To confirm the change of downstream apoptotic genes, classical proteins involved in apoptosis, such as Caspase-3 and Caspase-9, were measured 4 weeks after DEN treatment (Fig. 6C). NCoR1 deficiency slightly increased expression of Caspase-3 and Caspase-9 as well as their cleaved forms in PBS treatment, whereas DEN treatment significantly up-regulated their expression, especially the cleaved forms of Caspase-3 and Caspase-9, in *NCoR1*$^{\Delta hep}$ mice, whereas orlistat treatment significantly attenuated these differences between the two mouse groups (Fig. 6C). Together, these data indicate that there were more NADPH consumption, oxidative stress, and cell apoptosis induced after DEN treatment in *NCoR1*$^{\Delta hep}$ mice, compared to *NCoR1*$^{fl/fl}$ mice, which may have resulted from enhanced *de novo* FAS in the NCoR1 deficiency setting. Persistent cell apoptosis at the early stage of DEN treatment in *NCoR1*$^{\Delta hep}$ mice, but not in *NCoR1*$^{fl/fl}$ mice, may facilitate the clearance of proneoplastic lesions.

Discussion

This study characterized a distinct role of NCoR1 in the process of LR and carcinogenesis. Our results showed that significant differences exist in the restoration of liver/body weight ratio and the expression of cell-cycle-related proteins between *NCoR1*$^{fl/fl}$ and *NCoR1*$^{\Delta hep}$ mice following two-thirds PH. During the process of LR, 0–24 hours after two-thirds PH was identified as the metabolic phase with no significant hepatocyte proliferation, whereas 40–48 hours post-two-thirds PH[19] was nominated as the proliferation phase with much higher expression of Cyclin A2, a cell-cycle marker of mitosis, and Ki67 in *NCoR1*$^{\Delta hep}$ mice. In the metabolic phase, the significantly increased expression of Cyclin D1, a marker

of the G1 phase, was observed in *NCoR1*$^{\Delta hep}$ mice, indicating that the abnormal expression of Cyclin D1 and material preparation of cell-cycle entry is indispensable for enhanced regenerative capacity. More hepatocytes will enter the G1 phase and undergo cell mitosis because the expression of Cyclin A2 was enhanced 48 hours after two-thirds PH in *NCoR1*$^{\Delta hep}$ mice. Some recent studies documented that Cyclin D1 takes its place in metabolic activation independent of the cell cycle.[20] Cyclin D1 could cooperate with cyclin-dependent kinase 4 and bind to the promoter of PPAR gamma, coactivator 1 α,[21] a metabolic activated factor. In our cytological study, proliferative rate was not influenced by *NCoR1* knockdown, but reduced under the condition of lipid deprivation plus *NCoR1* knockdown. These results suggest that faster recovery at the early stage of LR in *NCoR1*$^{\Delta hep}$ mice may be mainly associated with energy reserve for cell-cycle entry.

Lipid metabolism was reported to be indispensable for the initiation of LR.[13] Many regulators of peripheral lipid mobilization and formation of lipid droplets were also reported to participate in LR, such as farnesoid X receptor, caveolin-1, and PPARs.[13,22,23] PPARs belong to the super nuclear receptor family and mainly perform their functions in lipid metabolism. As a comprehensive nuclear receptor repressor gene, NCoR1 might affect lipid metabolism through this pathway. As expected, in the NCoR1 deficient setting, the downstream β-oxidation-related genes and FAS-related genes of PPARα are significantly up-regulated (Supporting Fig. S4A). This result suggested that activation of PPARα might accelerate lipid metabolism in *NCoR1*$^{\Delta hep}$ mice. After administering GW6471, a specific PPARα antagonist (Supporting Fig. S4B), we performed a two-thirds PH in both groups. An obvious difference of liver/body ratio between NCoR1-WT and NCoR1-CKO mice was still observed after administration of GW6471 (Supporting Fig. S4C,D), and no obvious changes were found in NCoR1-WT mice after two-thirds PH in the presence or absence of GW6471 (data not shown). Similar results were observed by Oil Red O staining and IHC analysis of Ki67 (Supporting Fig. S4E,F). Bioinformatics analysis of the differentially expressed genes between *NCoR1*$^{fl/fl}$ and *NCoR1*$^{\Delta hep}$ mice at the early phase after two-thirds PH (Fig. 2D) revealed that the key enzymes of *de novo* FAS, such as FASN and ACC2, hit their expression peaks at the initial time before PH in *NCoR1*$^{\Delta hep}$ mice but 24 hours after PH in *NCoR1*$^{fl/fl}$ mice. NCoR1 was degraded quickly after two-thirds PH by the proteasome pathway.[24] Given that the phosphorylation of ACC1 and ACC2 induced by lipid-activated AMP-activated protein kinase (AMPK) signaling could be degraded by the proteasome pathway,[15] the down-regulation of these enzyme in *NCoR1*$^{\Delta hep}$ mice at 24 hours after PH may have resulted from feedback of fast lipid drop accumulation and AMPK activation. Furthermore, interfering with *de novo* FAS by pretreatment with orlistat hampered lipid accumulation and slowed down the regeneration rate of liver mass after two-thirds PH in both mice groups. The proliferative rate of HCC cell lines was not influenced by *NCoR1* knockdown, but reduced under the condition of exogenous lipid deprivation plus *NCoR1* knockdown. That means that *NCoR1* knockdown enhanced endogenous FAS to provide lipids for cell proliferation.

We suggest that *de novo* FAS in the G1 phase after two-thirds PH is different from *de novo* FAS in physical conditions. FASN and ACC2 are rate-limiting enzymes for *de novo* FAS. Furthermore, FASN plays a key role in many processes of lipid synthesis and coordinates with ACC1 and ACC2.[25–27] Here, we used orlistat, a selective FASN inhibitor, as an

intervention. Other selective inhibitors targeting *de novo* FAS may be used in our future work. We found that ACC2, a specific rate-limiting enzyme in *de novo* FAS, was up-regulated in livers of $NCoR1^{fl/fl}$ mice at 24 hours after two-thirds PH. ACC2 is normally expressed in myocytes and adipocytes, but not in hepatocytes, whereas ACC1 is mainly expressed in hepatocytes. ACC2 is located at the mitochondrial membrane, but ACC1 is located in the cytoplasm. ACC2 could inhibit CPT1 more efficiently than ACC1 given that malonyl-CoA generated by ACC2 at the surface of the mitochondria could directly inhibit CPT1 and shut down the delivery of fatty acids destined for oxidation.[26] In $NCoR1^{\Delta hep}$ mice, up-regulation of ACC2 was observed at time 0, suggesting that early preparation for enhanced *de novo* FAS was underway. Increased expression of ACC2 could be the main cause for lipid accumulation, which was reported to be crucial for initiation of mitosis. Interestingly, the peak of NCoR1 expression appears in *Fasn* and *Acc2* genes both in day and night (10:00 AM and 10:00 PM) according to the ChIP-seq results. Those data suggested that NCoR1 acts as a repressor in the expression of *Fasn*, *Acc2*, or other genes involved in lipid metabolism in quiescent hepatocytes. NCoR1 was normally expressed in liver and sharply down-regulated at 24 hours after two-thirds PH. This down-regulation of protein level is faster than mRNA change and probably is related to proteasome degradation.[24] NCoR1 was known to bind to the PPARs/CCAAT enhancer binding proteins complex for regulation of metabolism, and any changes in this complex have been shown to impact PPARs and their target genes.[9] The existence of NCoR1 and HDACs limits the stress-related or tissue-specific responses of nuclear receptors to certain ligands by histone deacetylation.[9,24] Deficiency of NCoR1 in hepatocytes may down-regulate the threshold of gene expression, so the G1 phase-specific genes could be expressed without stimuli.

Hypermetabolism and the enhanced capacity of glucose uptake are associated with malignant transformation. Attenuation of tumorigenic lesions in $NCoR1^{\Delta hep}$ mice was observed 36 weeks after DEN treatment. It seemed that the *de novo* FAS in the presence of NCoR1 prevents liver carcinogenesis, which is different from lipid accumulation during NASH. It is well known that NASH was demonstrated to be tumor promoting, but NASH is caused by a model with sustained supplying of a high-fat diet in a passive way.[27] Besides, the utilization of glucose and fatty acids in liver with NASH is also hampered, which is induced by oxidative stress and sustained inflammation. However, NCoR1 deficiency increases *de novo* FAS and glucose uptake in a positive way, and the mitochondrial function is enhanced. Collectively, exogenous lipid is important for LR, but it could bring about steatohepatitis and the hazard of oncogenesis. Although *de novo* FAS is also regenerative promoting, it is protective for carcinogenesis.

Considering that improved regenerative capacity and carcinogenesis are positively correlated, the question arises of how NCoR1 mediates the balance between compensatory proliferation and carcinogenesis by affecting *de novo* FAS. PH is acute with larger numbers of hepatocyte loss, whereas DEN injury is chronic with a prolonged DNA damage. Sustained *de novo* FAS could break redox state homeostasis, given that *de novo* FAS consumes glucose and NADPH, which is a reducing agent required for the production of reduced glutathione and glutathione peroxidase activity to eliminate intracellular ROS. Enhanced *de novo* FAS was correlated with the up-regulation of G6PD, a key enzyme of PPP (Fig. 2F). This indicates that a high level of G6PD in $NCoR1^{\Delta hep}$ mice could be

compensatory for maintenance of redox homeostasis. In addition, DNA damage after DEN administration could induce mitochondrial-dependent apoptosis by increasing mitochondrial ROS. Failure to maintain NADPH levels in *NCoR1*$^{\Delta hep}$ mice could amplify apoptosis signaling after DNA damage as a result of insufficient reducing agent to eliminate ROS. However, two-thirds PH is an acute injury with short-term stimulus. The redox balance could be achieved quickly after the liver was fully restored. Thus, enhanced *de novo* FAS may facilitate cells to enter the cell cycle under the process of LR, but attenuate prolonged HCG (Fig. 7B). Consistent with another study, knockdown of ACC2 resulted in the increase of tumor formation.[15]

In conclusion, NCoR1 represses genes involved in lipid synthesis in quiescent hepatocytes (Fig. 7A). In an acute liver injury situation, NCoR1 deficiency could enhance *de novo* FAS and provide more energy for LR. However, in a chronic liver injury circumstance, such as the DEN-induced HCC model, failure to suppress FAS-related genes could result in sustained *de novo* FAS in *NCoR1*$^{\Delta hep}$ mice, which subsequently increases cell apoptosis and attenuates the formation of proneoplastic lesions (Fig. 7B).

Supplementary Material

Refer to Web version on PubMed Central for supplementary material.

Acknowledgments:

We acknowledge the members of the International Co-operation Laboratory on Signal Transduction, especially Dong-Ping Hu, Shan-Hua Tang, Lin-Na Guo, Dan Cao, Dan-Dan Huang, Liang Tang, and Shan-Na Huang, for excellent technical assistance.

Supported by the State Key Project for Liver Cancer (2012ZX10002–009), the National Research Program of China (2012CB316503, 2012AA02A201), the National Natural Science Foundation of China (81422032, 81672860, 81300306, 81372674, and 91529303), and the Science Foundation of Shanghai (134119a3700).

Abbreviations:

8-OHdG	8-hydroxy-2’-deoxyguanosine
AAV	adeno-associated virus
ACC	acetyl-CoA carboxylase
Acacb/Acc2	acetyl-CoA carboxylase 2
Alb	albumin
AMPK	AMP-activated protein kinase
ATP	adenosine triphosphate
ChlP-seq	chromatin immunoprecipitation sequencing
CPT1	carnitine palmitoyltransferase 1
DEN	diethylnitrosamine

DMEM	Dulbecco's modified Eagle's medium
FAO	fatty acid β-oxidation
FAS	fatty acid synthesis
FASN	fatty acid synthase
FBS	fetal bovine serum
G6PD	glucose-6-phosphate dehydrogenase
GLUT	glucose transport type
GSH	glutathione
GSSG	glutathione disulfide
HCC	hepatocellular carcinoma
HCG	hepatocarcinogenesis
HDAC3	histone deacetylase 3
H&E	hematoxylin-eosin
IHC	immunohistochemical
KAT8	lysine acetyltransferase 8
LR	liver regeneration
$NADP^+$	nicotinamide adenine dinucleotide phosphate
NADPH	$NADP^+$ reduced
NASH	nonalcoholic steatohepatitis
NCoR1	nuclear receptor corepressor 1
$NCoR1^{\Delta hep}$	NCoR1 liver-specific null mice
$NCoR1^{fl/fl}$	NCoR1-floxed mice
PAR4	protease-activated receptor 4
PBS	phosphate-buffered saline
PCNA	proliferating cell nuclear antigen
PH	partial hepatectomy
PPAR	peroxisome proliferator-activated receptor
PPP	pentose phosphate pathway
p-RB	retinoblastoma protein

ROS	reactive oxygen species
shRNA	small hairpin RNA
TG	triglyceride
TUNEL	(terminal deoxynucleotidyl transferase dUTP nick end labeling)

REFERENCES

1.) Shyh-Chang N, Zhu H, de Soysa Yvanka T, Shinoda G, Seligson MT, Tsanov KM, et al. Lin28 enhances tissue repair by reprogramming cellular metabolism. Cell 2013;155:778–792. [PubMed: 24209617]
2.) Pauta M, Rotllan N, Vales F, Fernandez-Hernando A, Allen RM, Ford DA, et al. Impaired liver regeneration in Ldlr$^{-/-}$ mice is associated with an altered hepatic profile of cytokines, growth factors, and lipids. J Hepatol 2013;59:731–737. [PubMed: 23712050]
3.) Bai H, Zhang N, Xu Y, Chen Q, Khan M, Potter JJ, et al. Yes-associated protein regulates the hepatic response after bile duct ligation. Hepatology 2012;56:1097–1107. [PubMed: 22886419]
4.) Goldenberg D, Eferl R. p21Waf1/Cip1 revisited: oncogenic function in hepatocellular carcinoma. Gut 2014;63:1372–1373. [PubMed: 24221458]
5.) Malato Y, Ehedego H, Al-Masaoudi M, Cubero FJ, Bornemann J, Gassler N, et al. NF-kappaB essential modifier is required for hepatocyte proliferation and the oval cell reaction after partial hepa-tectomy in mice. Gastroenterology 2012;143:1597–1608.e.11. [PubMed: 22922425]
6.) Nouet Y, Dahan J, Labalette C, Levillayer F, Julien B, Jouvion G, et al. The four and a half LIM-only protein 2 regulates liver homeostasis and contributes to carcinogenesis. J Hepatol 2012; 57:1029–1036. [PubMed: 22796152]
7.) Zhang D, Cho E, Wong J. A critical role for the co-repressor N-CoR in erythroid differentiation and heme synthesis. Cell Res 2007;17:804–814. [PubMed: 17768398]
8.) Alenghat T, Meyers K, Mullican SE, Leitner K, Adeniji-Adele A, Avila J, et al. Nuclear receptor corepressor and histone deacetylase 3 govern circadian metabolic physiology. Nature 2008;456: 997–1000. [PubMed: 19037247]
9.) Sun Z, Feng D, Fang B, Mullican SE, You SH, Lim HW, et al. Deacetylase-independent function of HDAC3 in transcription and metabolism requires nuclear receptor corepressor. Mol Cell 2013;52:769–782. [PubMed: 24268577]
10.) Mottis A, Mouchiroud L, Auwerx J. Emerging roles of the corepressors NCoR1 and SMRT in homeostasis. Genes Dev 2013; 27:819–835. [PubMed: 23630073]
11.) Perissi V, Jepsen K, Glass CK, Rosenfeld MG. Deconstructing repression: evolving models of co-repressor action. Nat Rev Genet 2010;11:109–123. [PubMed: 20084085]
12.) Yamamoto H, Williams EG, Mouchiroud L, Canto C, Fan W, Downes M, et al. NCoR1 is a conserved physiological modulator of muscle mass and oxidative function. Cell 2011;147:827–839. [PubMed: 22078881]
13.) Borude P, Edwards G, Walesky C, Li F, Ma X, Kong B, et al. Hepatocyte-specific deletion of farnesoid X receptor delays but does not inhibit liver regeneration after partial hepatectomy in mice. Hepatology 2012;56:2344–2352. [PubMed: 22730081]
14.) Maehara Y, Fernandez-Checa JC. Augmenter of liver regeneration links mitochondrial function to steatohepatitis and hepatocellular carcinoma. Gastroenterology 2015;148:285–288. [PubMed: 25529802]
15.) Jeon SM, Chandel NS, Hay N. AMPK regulates NADPH homeostasis to promote tumour cell survival during energy stress. Nature 2012;485:661–665. [PubMed: 22660331]
16.) Li P, Fan W, Xu J, Lu M, Yamamoto H, Auwerx J, et al. Adipocyte NCoR knockout decreases PPARgamma phosphorylation and enhances PPARgamma activity and insulin sensitivity. Cell 2011;147:815–826. [PubMed: 22078880]

17.) Freimuth J, Bangen JM, Lambertz D, Hu W, Nevzorova YA, Sonntag R, et al. Loss of caspase-8 in hepatocytes accelerates the onset of liver regeneration in mice through premature nuclear factor kappa B activation. HEPATOLOGY 2013;58:1779–1789. [PubMed: 23728913]
18.) Lin HP, Cheng ZL, He RY, Song L, Tian MX, Zhou LS, et al. Destabilization of fatty acid synthase by acetylation inhibits de novo lipogenesis and tumor cell growth. Cancer Res 2016;76: 6924–6936. [PubMed: 27758890]
19.) Kohjima M, Tsai TH, Tackett BC, Thevananther S, Li L, Chang BH, Chan L. Delayed liver regeneration after partial hepatectomy in adipose differentiation related protein-null mice. J Hepatol 2013;59:1246–1254. [PubMed: 23928401]
20.) Shupe TD, Petersen BE. Liver regeneration: a consequence ofcom-plex, well-orchestrated signals. HEPATOLOGY 2015;62:644–645. [PubMed: 25953495]
21.) Bhalla K, Liu WJ, Thompson K, Anders L, Devarakonda S, Dewi R, et al. Cyclin D1 represses gluconeogenesis via inhibition of the transcriptional coactivator PGC1alpha. Diabetes 2014;63:3266–3278. [PubMed: 24947365]
22.) Fernandez-Rojo MA, Restall C, Ferguson C, Martel N, Martin S, Bosch M, et al. Caveolin-1 orchestrates the balance between glucose and lipid-dependent energy metabolism: implications for liver regeneration. HEPATOLOGY 2012;55:1574–1584. [PubMed: 22105343]
23.) Zhang L, Wang YD, Chen WD, Wang X, Lou G, Liu N, et al. Promotion of liver regeneration/ repair by farnesoid X receptor in both liver and intestine in mice. HEPATOLOGY 2012;56:2336–2343. [PubMed: 22711662]
24.) Jo YS, Ryu D, Maida A, Wang X, Evans RM, Schoonjans K, Auwerx J. Phosphorylation of the nuclear receptor corepressor 1 by protein kinase B switches its corepressor targets in the liver in mice. Hepatology 2015;62:1606–1618. [PubMed: 25998209]
25.) Marjanovic J, Chalupska D, Patenode C, Coster A, Arnold E, Ye A, et al. Recombinant yeast screen for new inhibitors of human acetyl-CoA carboxylase 2 identifies potential drugs to treat obesity. Proc Natl Acad Sci U S A 2010;107:9093–9098. [PubMed: 20439761]
26.) Oh W, Abu-Elheiga L, Kordari P, Gu Z, Shaikenov T, Chirala SS, Wakil SJ. Glucose and fat metabolism in adipose tissue of acetyl-CoA carboxylase 2 knockout mice. Proc Natl Acad Sci U S A 2005;102:1384–1389. [PubMed: 15677334]
27.) Chan CB, Tse MC, Liu X, Zhang S, Schmidt R, Otten R, et al. Activation of muscular TrkB by its small molecular agonist 7,8-dihydroxyflavone sex-dependently regulates energy metabolism in diet-induced obese mice. Chem Biol 2015;22:355–368. [PubMed: 25754472]
28.) Gazit V, Weymann A, Hartman E, Finck BN, Hruz PW, Tzekov A, Rudnick DA. Liver regeneration is impaired in lipo-dystrophic fatty liver dystrophy mice. HEPATOLOGY 2010;52: 2109–2117. [PubMed: 20967828]

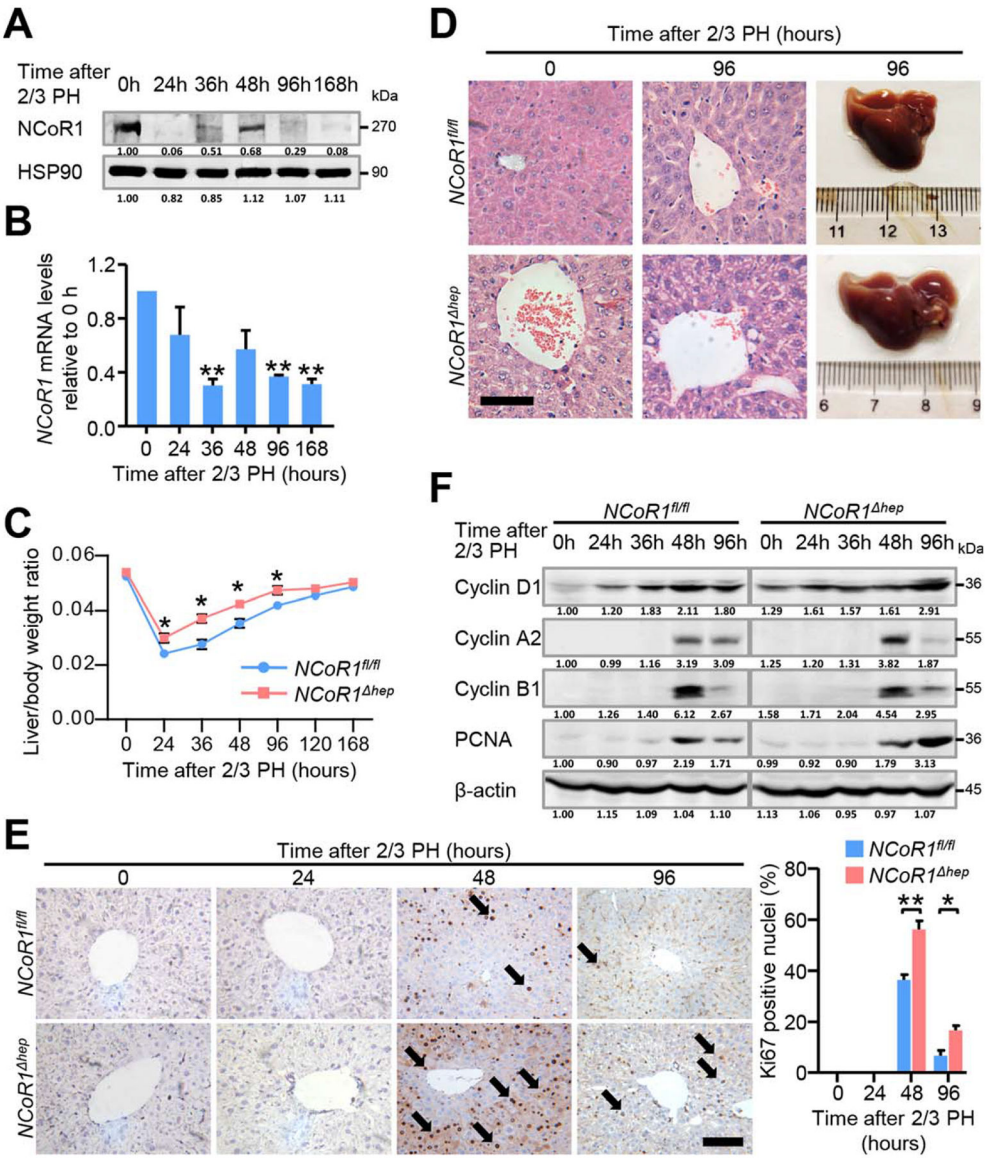

FIG. 1.

Liver regeneration after 2/3 partial hepatectomy is enhanced in *NCoR1*$^{\Delta hep}$ mice. (A) Protein and (B) mRNA expression change of NCoR1 in the process of liver regeneration were detected by western blot and qPCR, Data are presented as mean ± SEM (n=4). **P*<0.05; ***P*<0.01. (C) Liver weight to body weight ratio analysis in *NCoR1*$^{fl/fl}$ and *NCoR1*$^{\Delta hep}$ mice over a time course from 0 to 168 hours after 2/3 PH. Data are presented as mean ± SEM (n=5). **P*<0.05; ***P*<0.01, *NCoR1*$^{\Delta hep}$ mice compared to *NCoR1*$^{fl/fl}$ mice at the indicated times. (D) Morphological changes of livers of *NCoR1*$^{fl/fl}$ mice and *NCoR1*$^{\Delta hep}$ mice at the 96 hours after 2/3 PH as determined by H&E staining. scale bar: 50 μm. (E) Immunohistochemical analysis of Ki67 in paraffin tissues from livers of *NCoR1*$^{fl/fl}$ and *NCoR1*$^{\Delta hep}$ mice at the indicated times after 2/3 PH (Left). Quantification of the percentage of Ki67 labeled nuclei (Right). Data are presented as mean ± SEM (n=4). The different degrees of significance were indicated as follows in the graphs: **P*<0.05, ***P*<0.01,

NCoR1$^{\Delta hep}$ mice compared to *NCoR1*$^{fl/fl}$ at indicated time. (F) Western blot analysis of CyclinD1, CyclinA2, CyclinB1, PCNA using RIPA extracts of *NCoR1*$^{fl/fl}$ and *NCoR1*$^{\Delta hep}$ livers obtained at the indicated times after 2/3 PH. (Two Way ANOVA plus Student's t test for B, C; Student's t test for E).

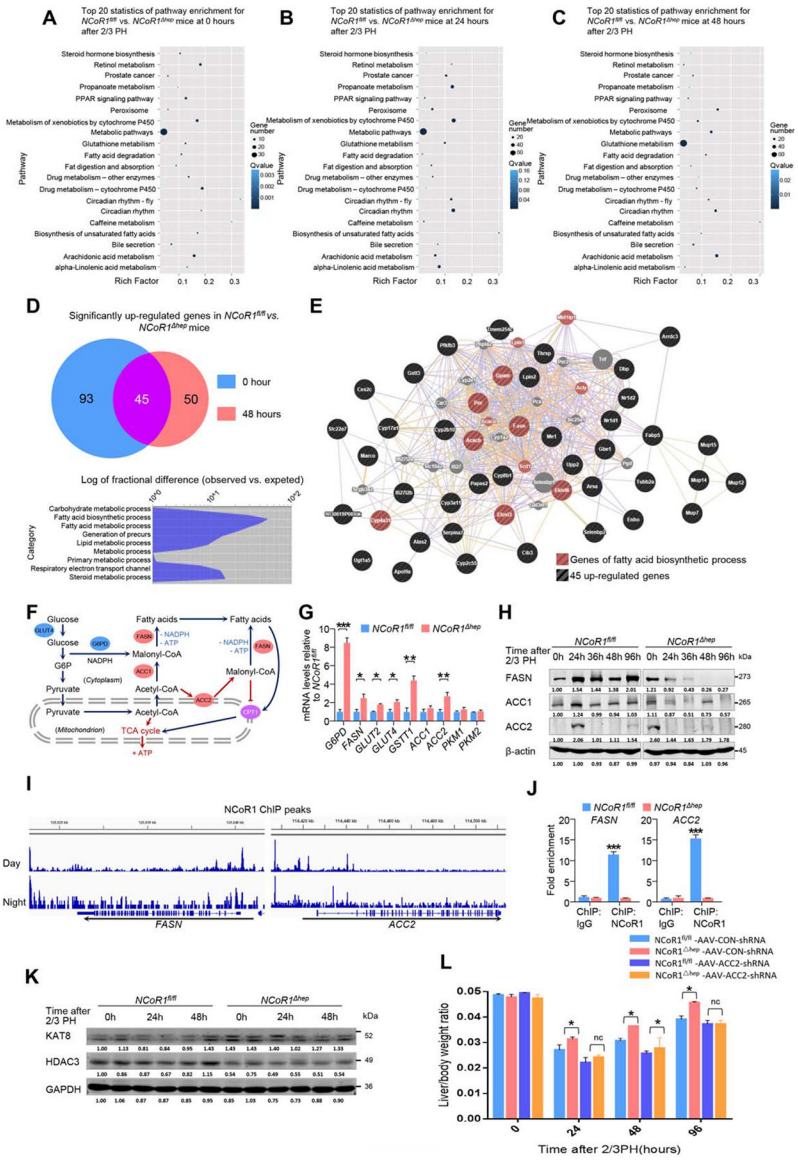

FIG. 2.

Bioinformatic analysis of specific genes for NCoR1 regulating compensatory proliferation. (A-C) A transcriptome re-sequencing of RNA from *NCoR1*$^{fl/fl}$ and *NCoR1*$^{\Delta hep}$ mouse liver samples at 0 hours, 24 hours and 48 hours. Pathway analysis of differentially-expressed genes between *NCoR1*$^{fl/fl}$ and *NCoR1*$^{\Delta hep}$ mice are displayed at the indicated times. (D) Functional analysis of genes upregulated at 0 hours and 48 hours. (E) Gene co-expression network of the 45 up-regulated genes are displayed. (F) Schematic diagram of *de novo* FAS: fatty acids could be produced in liver from glucose or acetyl-CoA. The rate-limiting enzyme are FASN, ACC1 and ACC2. Fatty acids could also be used to produce ATP through CPT1, which could be effectively inhibited by ACC2 regulated malonyl-CoA. The production of fatty acids is ATP consumption and NADPH consumption, which is produced from PPP pathway. (ACC, acetyl-CoA carboxylase; FASN, fatty acid synthase; G6PD, glucose-6-phosphate dehydrogenase; CPT1, carnitine palmitoyl transterase-1). (G) qPCR analysis of

mRNAs of the glucose metabolism genes *Glut2*, *Glut4*, *Pkm1*, *Pkm2* and *G6pd*; lipid synthesis genes *Fasn*, *Acc1*, *Acc2*, redox state-related gene *Gstt1* at the 0 time point in $NCoR1^{fl/fl}$ and $NCoR1^{\Delta hep}$ mice are presented. Data are presented as mean ± SEM (n=4). *P<0.05, **P<0.01, $NCoR1^{\Delta hep}$ mice compared to $NCoR1^{fl/fl}$ mice. (H) Western blot analysis of expression change of FASN, ACC1 and ACC2 protein levels at the indicated time points after 2/3 PH. (I) ChIP-seq results of NCoR1 binding sites in *Fasn* and *Acc2* genes during the day (10 am) and night (10 pm). (J) ChIP-qPCR results using anti-NCoR1 antibody and anti-IgG antibody for *Fasn* and *Acc2*. Data are presented as mean ± SEM (n=3). ***P<0.001, $NCoR1^{\Delta hep}$ mice compared to $NCoR1^{fl/fl}$ mice. (K) Western blot analysis of expression change of KAT8 and HDAC3 protein levels at the indicated time points after 2/3 PH. (L) Liver weight to body weight ratio analysis in $NCoR1^{fl/fl}$ and $NCoR1^{\Delta hep}$ mice over a time course from 0 to 96 hours after 2/3 PH. Data are presented as mean ± SEM (n=5). *P<0.05; **P<0.01, $NCoR1^{\Delta hep}$ mice compared to $NCoR1^{fl/fl}$ mice at the indicated times. (Student's t test for G/J/L).

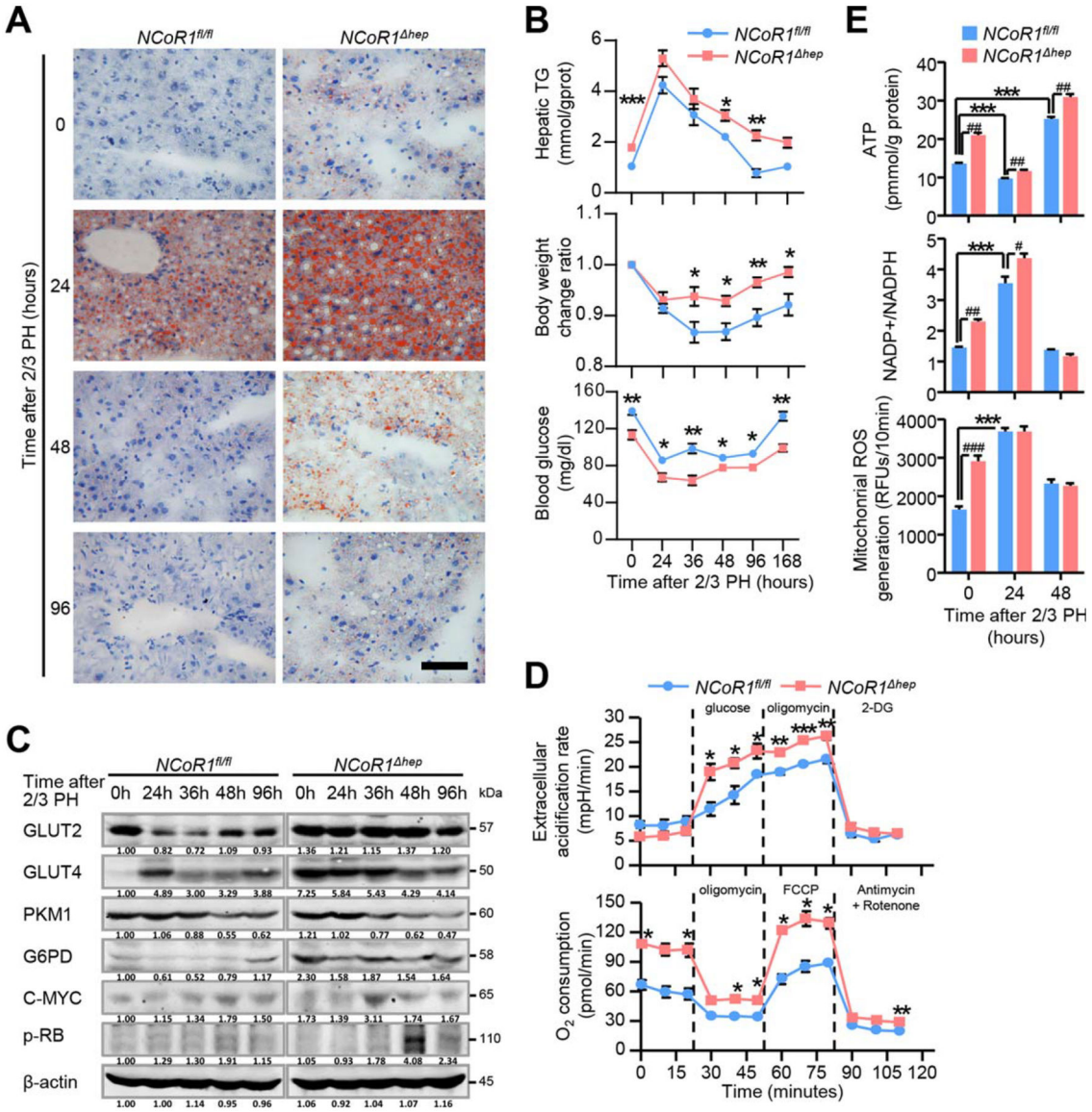

FIG. 3.

Enhanced glucose flux, mitochondrial function and *de novo* FAS genesis in *NCoR1*$^{\Delta hep}$ mice at the early stages of liver regeneration after 2/3 PH. (A) Analysis of the lipids by Oil Red O staining performed with frozen liver sections. scale bar: 50 μm (B) Analysis of liver triglyceride (TG) contents, body weight change ratios and serum glucose in *NCoR1*$^{fl/fl}$ and *NCoR1*$^{\Delta hep}$ mice at the indicated time points after 2/3 PH. Data are presented as mean ± SEM (n=5). The different degrees of significance were indicated as follows in the graphs: **P*<0.05; ***P*<0.01, *NCoR1*$^{\Delta hep}$ mice compared to *NCoR1*$^{fl/fl}$ mice. (C) Western blot analysis of expression change of protein level of GLUT2, GLUT4, PKM1, G6PD, C-MYC and p-RB at the indicated time points after PH. (D) Upper panel: Extracellular acidification rate (ECAR) of *NCoR1*$^{fl/fl}$ and *NCoR1*$^{\Delta hep}$ primary hepatocytes, as measured by the Seahorse Analyzer (n = 4 each). Addition of glucose induces glycolysis-dependent lactic acid production and ECAR. Oligomycin then induces maximal ECAR, and 2-DG partially

inhibits glycolysis-dependent ECAR. Lower panel: Oxygen consumption rate (OCR) of *NCoR1*$^{fl/fl}$ and *NCoR1*$^{\Delta hep}$ primary hepatocytes, as measured by the Seahorse Analyzer (n = 4 each). Oligomycin treatment inhibits ATP synthase dependent OCR. The proton gradient uncoupler FCCP then induces maximal OCR, and antimycin/rotenone finally inhibits all OxPhos-dependent OCR. *P<0.05; **P<0.01, ***P<0.001, *NCoR1* KO hepatocyte compared to *NCoR1*$^{fl/fl}$ hepatocyte. (E) Biochemical detection of intracellular ATP levels, NADP+/NADPH ratios and mitochondrial ROS in *NCoR1*$^{fl/fl}$ and *NCoR1*$^{\Delta hep}$ mice at the indicated times after 2/3 PH. Data are presented as mean ± SEM (n=4). The different degrees of significance were indicated as follows in the graphs: *P<0.05; **P<0.01; ***P<0.001, *NCoR1*$^{fl/fl}$ mice at 0 hours compared with *NCoR1*$^{fl/fl}$ mice at indicated times after 2/3 PH. $^{\#}P$<0.05; $^{\#\#}P$<0.01, $^{\#\#\#}P$<0.001, *NCoR1*$^{\Delta hep}$ mice compared to *NCoR1*$^{fl/fl}$ mice at indicated times after 2/3 PH. (Two Way ANOVA plus Student's t test for B, D; Student's t test for E).

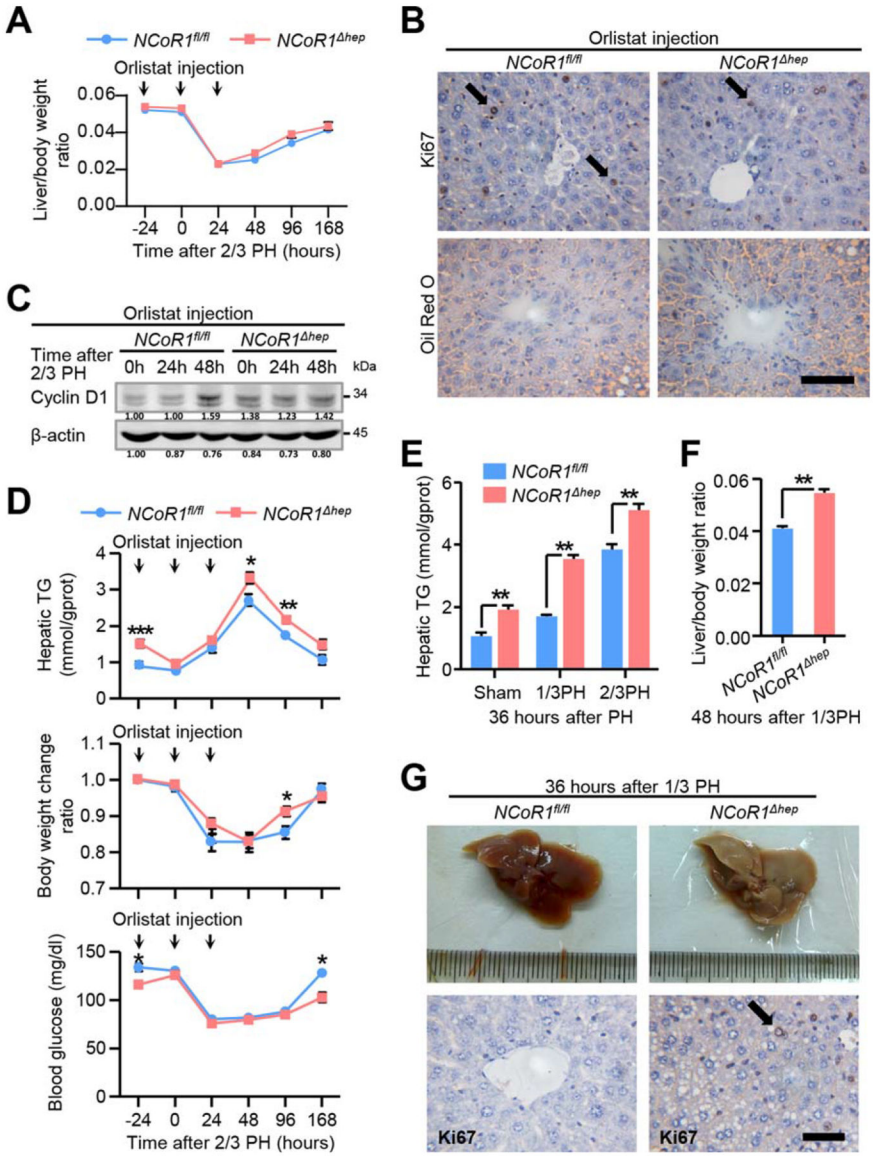

FIG. 4.

Enhanced *de novo* FAS facilitate compensatory proliferation after 2/3 PH and alters the metabolic state in liver. (A) Liver to body weight ratio analysis in *NCoR1*$^{fl/fl}$ and *NCoR1*$^{\Delta hep}$ mice over a time course from 0 to 168 hours after 2/3 PH and pretreated with orlistat from 24 hours before to 24 hours after 2/3 PH in a daily pattern, Data in are presented as mean ± SEM (n=5). (B) Immunohistochemical analysis of Ki67 in paraffin tissues from liver of *NCoR1*$^{fl/fl}$ and *NCoR1*$^{\Delta hep}$ mice at 48 hours after 2/3 PH and Oil Red O staining of frozen sections from livers of *NCoR1*$^{fl/fl}$ and *NCoR1*$^{\Delta hep}$ mice at 24 hours after 2/3 PH, which were pretreated with orlistat. scale bar: 50 μm. (C) Western blot analysis of CyclinD1 using RIPA extracts of *NCoR1*$^{fl/fl}$ and *NCoR1*$^{\Delta hep}$ livers obtained at the early stage after 2/3 PH. (D) Analysis of liver triglyceride (TG) content, body weight change ratio and serum glucose at indicated time points in *NCoR1*$^{fl/fl}$ and *NCoR1*$^{\Delta hep}$ mice pretreated with orlistat from 24 hours before to 24 hours after 2/3 PH, Data in are presented as mean ±

SEM (n = 5). The different degrees of significance were indicated as follows in the graphs: **P*<0.05; ***P*<0.01, *NCoR1*$^{fl/fl}$ mice compared to WT mice. (E) Biochemical detection of liver triglyceride content in *NCoR1*$^{fl/fl}$ and *NCoR1*$^{\Delta hep}$ mice at 36 hours after sham surgery, 1/3 PH or 2/3 PH. Data in are presented as mean ± SEM (n=5). ***P*<0.01, *NCoR1*$^{\Delta hep}$ mice compared to *NCoR1*$^{fl/fl}$ mice. (F) Analysis of the liver/body weight ratio of *NCoR1*$^{fl/fl}$ and *NCoR1*$^{\Delta hep}$ mice at 48 hours after 1/3 PH. Data in are presented as mean ± SEM (n=4). The different degrees of significance are indicated as follows in the graphs: ***P*<0.01, *NCoR1*$^{\Delta hep}$ mice compared to *NCoR1*$^{fl/fl}$ mice. (G) Morphological change of livers of *NCoR1*$^{fl/fl}$ mice and *NCoR1*$^{\Delta hep}$ mice at the 36 hours after 1/3 PH; Immunohistochemical analysis of Ki67 in paraffin tissues from liver of *NCoR1*$^{fl/fl}$ and *NCoR1*$^{\Delta hep}$ mice at the same time. scale bar: 50 μm. (Two Way ANOVA plus Student's t test for A, D; Student's *t* test for E, F).

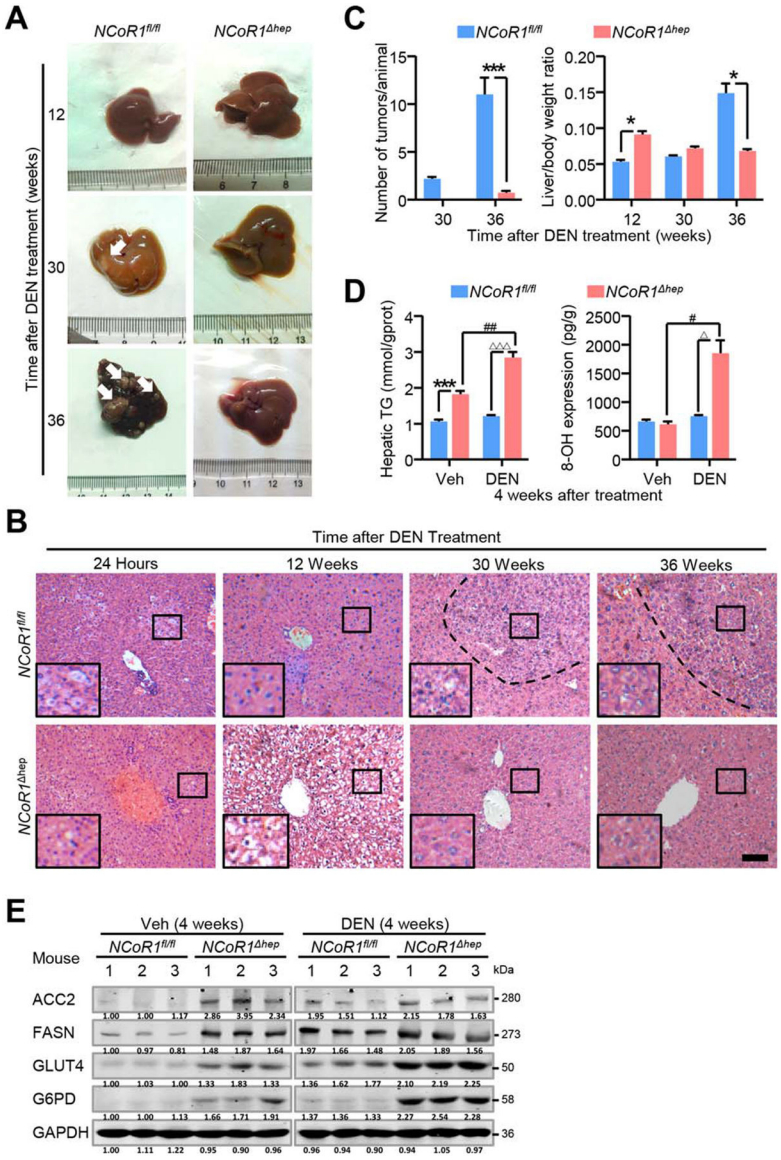

FIG. 5.

Attenuated formation of DEN-induced tumors in *NCoR1*$^{\Delta hep}$ mice. (A) *NCoR1*$^{fl/fl}$ and *NCoR1*$^{\Delta hep}$ mice were intraperitoneally injected with PBS or DEN at day 15 after born and livers collected at 24 hours after injection and 4, 12, 30, 36 weeks after injection. Representative images and (B) representative H&E histological features of livers from DEN-treated mice at the indicated times after killing were shown. scale bar: 100 μm. (C) Quantification of the number of macroscopic tumors per animal and analysis of the liver to body weight ratio of *NCoR1*$^{fl/fl}$ and *NCoR1*$^{\Delta hep}$ mice. Data are presented as mean ± SEM (n=5). The different degrees of significance are indicated as follows in the graphs: **P*<0.05; ****P*<0.001, *NCoR1*$^{\Delta hep}$ mice compared to *NCoR1*$^{fl/fl}$ mice. (D) Biochemical detection of liver triglyceride content and 8-OhDG (8-OH) in *NCoR1*$^{fl/fl}$ and *NCoR1*$^{\Delta hep}$ mice treated with PBS or DEN at four weeks after injection. Data are presented as mean ± SEM (n=4). ****P*<0.001, *NCoR1*$^{\Delta hep}$ mice compared to *NCoR1*$^{fl/fl}$ mice treated with Veh. $^{\#}$*P*<0.05;

$^{\#\#}P<0.01$ $NCoR1^{\Delta hep}$ mice treated with Veh compared to $NCoR1^{\Delta hep}$ mice treated with DEN. $^{\Delta\Delta\Delta}P<0.001$, $NCoR1^{fl/fl}$ mice treated with DEN compared to $NCoR1^{\Delta hep}$ mice treated with DEN. (E) Western blot analysis of expression of protein level of ACC2, GLUT4, FASN, G6PD in $NCoR1^{fl/fl}$ and $NCoR1^{\Delta hep}$ mice treated with PBS or DEN at four weeks after DEN treatment. (Student's *t* test for B, D).

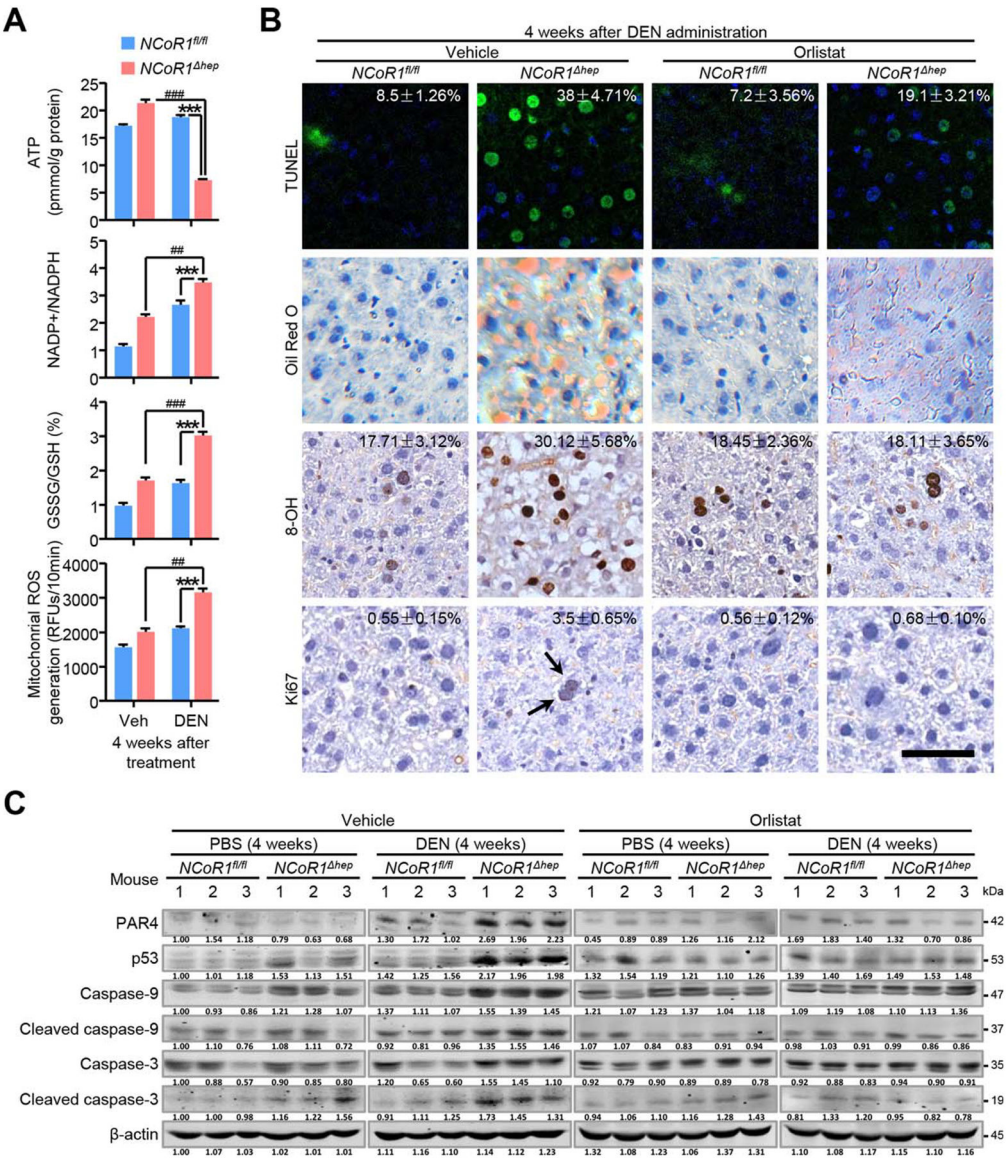

FIG. 6.

Increased oxidative stress and apoptosis in early stage of DEN injury in *NCoR1*$^{\Delta hep}$ mice. (A) Biochemical detection of intracellular ATP levels, NADP+/NADPH ratios, GSSG/GSH ratios and mitochondrial ROS in *NCoR1*$^{fl/fl}$ and *NCoR1*$^{\Delta hep}$ mice treated with PBS or DEN at four weeks after DEN treatment. Data are presented as mean ± SEM (n=4). ***P<0.001, *NCoR1*$^{\Delta hep}$ mice treated with DEN compared to *NCoR1*$^{fl/fl}$ mice treated with DEN. ##P<0.01; ###P<0.001, *NCoR1*$^{\Delta hep}$ mice treated with DEN compared to *NCoR1*$^{\Delta hep}$ mice treated with control vehicle. (B) Four weeks after DEN administration, *NCoR1*$^{fl/fl}$ and *NCoR1*$^{\Delta hep}$ mice were treated with vehicle or orlistat for 5 days before sample collection. Representative Tunel staining, Oil Red O staining and immunohistochemical analysis of 8-OH and Ki67 were performed on mice liver samples. Quantification of the percentage of Tunel, 8-OH and Ki67 labeled nuclei were marked. Data are presented as meaňSEM of at least four mice per group. scale bar: 50 μm. (C) Four weeks after DEN administration,

NCoR1$^{fl/fl}$ and *NCoR1*$^{\Delta hep}$ mice were treated with vehicle or orlistat for 5 days. Western blot analysis of expression of protein level of p53, PAR4, Caspase-3 and Caspase-9 (full length and their cleaved form) in mice liver samples were performed. (Student's *t* test for A, B).

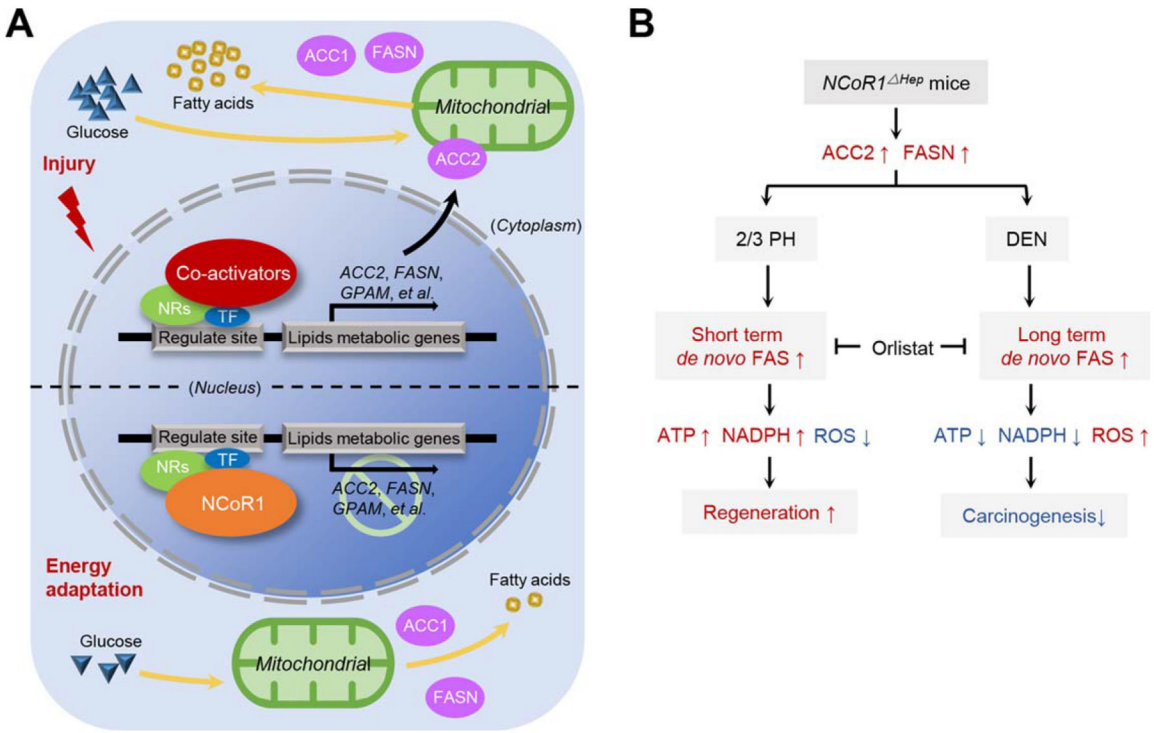

FIG. 7.

Schematic representation of *NCoR1*$^{\Delta hep}$ mice in compensatory prolifaeration and DEN induced hepatocarcinogenesis. (A) Genes of specific lipid metabolism is up-regulated by the stimulation of injury in hepatocyte, such as *Acc2* and *Fasn*. NCoR1 epigenetically controls the expression of lipid metabolic genes when energy adaptation but is degraded in acute injury. (B) Distinct mechanism of *NCoR1*$^{\Delta hep}$ mice in compensatory proliferation and DEN induced hepatocarcinogenesis. PH is an acute injury with large number of hepatocyte loss. Deficiency of NCoR1 could facilitate a short-term *de novo* FAS to provide more lipid for energy supplement. While the redox balance could be achieved quickly after the liver was fully restored. DEN injury is chronical with a prolonged DNA damage. Sustained *de novo* FAS without NCoR1 control could consume more NADPH and enhance oxidative stress, which induce the mitochondrial-dependent apoptosis. Thus, the early neoplasia are hampered.